Original article

Changes in physiology, gene expression and ethylene biosynthesis in MDMV-infected sweet corn primed by small RNA pre-treatment

Kinga Balassa [a,*], György Balassa [a], Orsolya Kinga Gondor [b], Tibor Janda [b], Asztéria Almási [c], Szabolcs Rudnóy [a]

[a] Department of Plant Physiology and Molecular Plant Biology, Faculty of Science, Eötvös Loránd University, Budapest, Hungary
[b] Department of Plant Physiology, Agricultural Institute, Centre for Agricultural Research, ELKH Martonvásár, Hungary
[c] Department of Plant Pathology, Agricultural Institute, Centre for Agricultural Research, ELKH Budapest, Hungary

ABSTRACT

The physiological condition of plants is significantly affected by viral infections. Viral proliferation occurs at the expense of the energy and protein stores in infected plant cells. At the same time, plants invest much of their remaining resources in the fight against infection, making them even less capable of normal growth processes. Thus, the slowdown in the development and growth processes of plants leads to a large-scale decrease in plant biomass and yields, which may be a perceptible problem even at the level of the national economy. One form of protection against viral infections is treatment with small interfering RNA (siRNA) molecules, which can directly reduce the amount of virus that multiplies in plant cells by enhancing the process of highly conserved RNA interference in plants. The present work demonstrated how pre-treatment with siRNA may provide protection against MDMV (Maize dwarf mosaic virus) infection in sweet corn (*Zea mays* cv. *saccharata* var. Honey Koern). In addition to monitoring the physiological condition of the maize plants, the accumulation of the virus in young leaves was examined, parallel, with changes in the plant RNA interference system and the ethylene (ET) biosynthetic pathway. The siRNA pre-treatment activated the plant antiviral defence system, thus significantly reducing viral RNA and coat protein levels in the youngest leaves of the plants. The lower initial amount of virus meant a weaker stress load, which allowed the plants to devote more energy to their growth and development. In contrast, small RNA pre-treatment did not initially have a significant effect on the ET biosynthetic pathway, but later a significant decrease was observed both in the level of transcription of genes responsible for ET production and, in the amount of ACC (1-aminocyclopropane-1-carboxylic acid) metabolite. The significantly better physiological condition, enhanced RNAi response and lower quantity of virus particles in siRNA pretreated plants, suggested that siRNA pre-treatment stimulated the antiviral defence mechanisms in MDMV infected plants. In addition, the consistently lower ACC content of the plants pretreated with siRNA suggest that ET does not significantly contribute to the successful defence in this maize hybrid type against MDMV.
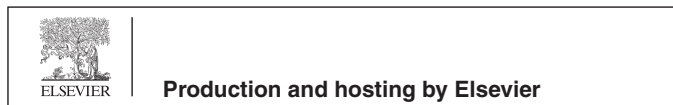
1. Introduction

The highly variable and often unpredictable weather currently experienced is in itself a burden on plant development and growth, and may also increase the susceptibility of plants to certain biotic stressors (e.g. viruses) (Yadav et al. 2019). At the same time, the rise in average temperatures caused by climate change may affect the pathogenicity of viruses, facilitating the spread of diseases to new areas, thereby contributing to the emergence of new epidemics (Trebicki 2020). Among the biotic stressors that threaten sweet corn, obligate intracellular parasitic viruses such as Maize dwarf mosaic virus (MDMV), which is widespread on a global scale, can be highlighted. The most characteristic symptom of MDMV infection is the chlorotic spots that appear at the base of the infected plant leaves in a mosaic pattern in early phenophases. Symptoms that appear later are manifested as dwarf growth and

yellow, chlorotic patches that form regular streaks (Wijayasekara and Ali 2020). Co-infection of MDMV which belongs to the Potyvirus genus, with other viruses often produces a synergistic effect that multiplies the symptoms of the disease, making it even more devastating. A good example of this is MLN (Maize lethal necrosis) disease, first registered in Kenya in 2011, the onset of which was due to co-infection with maize chlorotic mottle virus (MCMV) and MDMV, or other potyviruses (Kiruwa et al., 2019; Asiimwe et al., 2020). MDMV uses plant resources to enhance its own proliferation, thereby significantly contributing to the retardation of plant development and growth processes (Kannan et al. 2018). Thus, in the case of MDMV infection, plant biomass and yields are greatly reduced, resulting in global losses of up to $ 30 billion (Sastry and Zitter 2014). The primary plant defence strategy against viral infection is RNA interference (RNAi). The plant uses small RNA molecules complementary to the viral RNA to sequence-specifically cleave the viral nucleic acids, thus preventing their replication (Khraiwesh et al. 2012; Jin et al, 2021). Utilizing the working principle of this system, plant defence can be activated by treatment with longer double-stranded RNA molecules (dsRNAs) or shorter small RNA duplexes, mimicking the infection, but without real danger. Hence, it may ultimately be possible to slow down or even completely inhibit viral reproduction/replication/multiplication within the plant (Konakalla et al. 2016; Kaldis et al. 2018).

Plant phytohormones have a diverse and complex role in regulating plant growth and differentiation. However, they are also involved in the protection against abiotic and biotic stressors and mitigating stress damage. Salicylic acid, abscisic acid, jasmonic acid, and brassinosteroid plant hormones are able to help plant protection against various viral infections (Alazem and Lin 2015; Zhang et al. 2015), while quite different effects have been attributed to ethylene (ET) during various plant-virus interactions. There are two key enzymatic reactions in the ET biosynthetic pathway. First the substrate S-adenosyl-L-methionine (SAM) is converted to 1-aminocyclopropane-1-carboxylic acid (ACC) and 5′-methylthioadenosine (MTA) by the enzyme ACC synthase (ACS) (Adams and Yang 1977, 1979; Boller et al. 1979). Secondly the ACC is converted to ET, CO_2 and cyanide by the ACC oxidase enzyme (ACO) (Hamilton et al. 1991; Ververidis and John 1991). Both enzymes are under strict regulation, and their combined activity allows the precise regulation of ET production. Under normal circumstances, ACS is responsible for the rate limiting step, while more and more evidence points to the decisive role of ACO as well, for instance in stress (flooding) and also in growth and development (Houben and Van de Poel 2019). From the stress point of view the transcriptional and posttranslational regulation of these enzymes is mainly dependent on transcription factors linked to hormonal crosstalk (Pattyn et al., 2021). It has been suggested that ET plays a significant role in the development of protection against viral infection, while another concept is that ET is only involved in "crosstalk" within the hormonal network. Thus, it exerts its effect in collaboration with other hormones rather than regulating defence alone (Chen et al. 2013; Broekgaarden et al. 2015). In the case of Rice dwarf virus (RDV), an adverse ET effect on the plant was observed. As a result of infection, S-adenosylmethionine synthase (SAMS) activity in the ET biosynthetic pathway is directly stimulated, causing increased ET synthesis and increased susceptibility in rice plants (Zhao et al. 2017). The contradictory research results suggest that the role of ET may differ significantly in different plant-virus interactions depending on the type of plant and virus.

The present work demonstrated how siRNA pre-treatment may provide protection against MDMV infection, with special regard to the alteration of RNAi and ET biosynthesis.

2. Materials and methods

2.1. Plant material, growth conditions and treatments

Sweet corn (*Zea mays* cv. *Saccharata* var. Honey Koern.) was used to study the biosynthetic pathway of ET under biotic stress. Pregerminated corn grains were grown hydroponically on 1⁄4 strength Hoagland solution (which contained 80 µM Fe(III)-EDTA as the iron form). Plant growth was performed at 250 µmol photon m^{-2} s^{-1} PPFD, 23 ± 1 °C temperature and 50% relative humidity, in a SANYO MLR-350 HT (SANYO Electric Co., ltd., Japan) plant growth chamber with a 14/10 h light/dark period. Plants given no subsequent treatment were indicated as control (*Co*) plants. To investigate the effect of small RNA treatment on RNAi, 10 day old plants were treated with 21-nucleotide small interfering RNA (siRNA) molecules. In maize plants belonging to the *siRNA* group 10 µl of 30 ng/µl siRNA solution was pipetted the open leaf sheaths. The sequence of this siRNA (Table A.1) was identical to a 21-nt sequence in the 5′ part of the coat protein gene of reference MDMV genomes (AM490848, AM490849, FM883181, FM883202). We determined this sequence with small RNA sequencing of MDMV-infected sweet corn (unpublished). A maize MDMV model system was used to study biotic stress conditions. The first and second leaves of plants from the infected (*Inf*) group were inoculated with the Dallas A strain of MDMV on two occasions, 11 and 13 days after germination. 1 g leaf tissue with macroscopic symptoms from previously infected plants was homogenized in 10 mL Sörensen phosphate buffer (pH 7.2, 0.06 M) and used to inoculate the plant leaves. Carborundum was added as an abrasive. To investigate the effects of exogenous siRNA treatment in infected plants, siRNA pretreated plants were infected with MDMV Dallas A strain (*siRNA-Inf* group). Samples were collected at the same time on sampling days one, two and three weeks after the first MDMV inoculation (1, 2 and 3 wpi). Sampling for $\Delta F/F_m'$ measurements, virus quantification measurements, gene expression analysis and the metabolic measurement of ACC was performed throughout maize development, using the two youngest adult leaves each week. These were leaves 3 and 4 in the first week, leaves 4 and 5 in the second week, and leaves 5 and 6 in the third week. Chlorophyll content was examined from as many leaves as possible each week, thanks to the fact that the measurement is non-invasive. The F_v/F_m measurement was extended to leaves 3 and 4 in the second and third weeks and NPQ values were measured on leaves 4, 5 and 6 at 1, 2 and 3 wpi.

2.2. Measurement of chlorophyll content and basic growth parameters

The chlorophyll content of the plants was measured non-invasively with a SPAD-502Plus instrument (Konica Minolta, Tokyo, Japan). Measurements were taken from the same region of the 3rd, 4th, 5th, 6th and 7th leaves in each group. Examination of basic growth parameters included measurements of shoot and root length, and fresh and dry weight.

2.3. Chlorophyll a fluorescence measurements and investigation of non-photochemical quenching (NPQ) parameters

Chlorophyll *a* fluorescence was analysed on intact leaves using a PAM-101–102-103 fluorometer (Walz, Effeltrich, Germany) after

Table A1
Sequence of the small RNA molecule used in the (pre)treatment of the *siRNA* and *siRNA-Inf* groups. The sequence is identical to a 21-nt sequence in the 5′ part of the coat protein gene of reference MDMV genomes (AM490848, AM490849, FM883181, FM883202).

Sense:	Antisense:
5′−pGAAGCACAGAAGGAGGCAGAG−3′	5′−pCUGCCUCCUUCUGUGCUUCAG−3′

20 min of dark adaptation. The maximum quantum efficiency of PSII (F_v/F_m) was calculated from the values of minimal (F_0) and maximal fluorescence (F_m) as $F_v/F_m = (F_m-F_0)/F_m$. F_0 was determined by switching on the measuring light, with a modulation frequency of 1.6 kHz and PPFD of less than 1 μmol m^{-2} s^{-1}, after 3 s illumination with far-red light in order to eliminate reduced electron carriers. In the light-adapted state the actual quantum efficiency ($\Delta F/F_m'$) of photosystem II (PSII) was calculated from the values of the steady-state value (F_s) and maximal fluorescence (F_m'), as $\Delta F/F_m' = (F_m'-F_s)/F_m'$. The F_m and F_m' values were measured using a 0.7 s flash of white light at PPFD 3500 μmol mmol m^{-2} s^{-1} (light source: KL 1500 electronic, Schott, Mainz, Germany; Solti et al. 2008). For quenching analysis the leaves were exposed to actinic white light (PPFD of 100 mmol photons m^{-2}s^{-1}) for 20 min. Excitation energy allocations were calculated according to Hendrickson et al. (2005), where the parameters were: $\Phi_{f,D}$ – fluorescence and constitutive thermal dissipation; Φ_{NF} – thermal dissipation in non-functional PSII; Φ_{NPQ} – light-dependent and ΔpH- and xanthophyll-mediated thermal dissipation; Φ_{PSII} – PSII electron flow. The distribution of the parameters was calculated according to the following equation: $1 = \Phi_{PSII} + \Phi_{f,D} + \Phi_{NPQ} + \Phi_{NF}$.

2.4. Quantification of virus particles in the leaves of infected plants

Two methods were used to verify the success of infection and to determine the amount of virus in MDMV-infected plants. Viral coat protein quantities were determined with Double Antibody Sandwich (DAS) ELISA (Clark and Adams 1977), while viral RNA amounts were obtained using an absolute quantification RT-PCR method. MDMV coat protein was detected in maize leaves using an MDMV antiserum kit (Bioreba A.G., Reinach, Switzerland) following the manufacturer's instructions. Virus coat protein content was determined by photometric measurements at 405 nm with a Labsystem Multiskan MS spectrophotometer. The quantitation of viral RNA was performed by absolute quantification real-time PCR. For this purpose, an MDMV-specific PrimeTime probe (IDT Integrated DNA Technologies, Coralville, IA, USA) and GoTaq® Probe qPCR Master Mix (Promega, Madison, WI, USA) were used according to Ludmerszki et al. (2017).

2.5. Analysis of gene expression in maize

Total RNA was isolated from the leaves of maize plants using the Direct-zol RNA Miniprep Kit (Thermo Scientific, Rockford, IL, USA), including the DNA digestion step. cDNA was synthesised from 500 ng RNA with the RevertAid First Strand cDNA Synthesis Kit (Thermo Scientific, Rockford, IL, USA) with the use of random hexamer primers. RT-qPCR reactions were run on an ABI StepOne-Plus Real-Time PCR instrument (Thermo Fisher Scientific), using Maxima SYBR Green/ROX qPCR Master Mix (Thermo Fisher Scientific). Two housekeeping genes, *folylpolyglutamate synthase* (FPGS) and *leunig* (LUG) were used as internal control genes to normalize the Cq values of the studied genes. The geometric mean of the internal control data was applied for normalisation. The relative changes in gene expression were compared to the untreated control group and quantified according to the Pfaffl method (Pfaffl, 2004). Primers were designed with Primer3 online software (Koressaar and Remm, 2007) and fine-tuned manually if necessary. The prepared PCR reactions were optimized using gradient PCR. Reaction efficiencies were calculated with the LinRegPCR software (Ramakers et al. 2003). The gene expression assay included genes belonging to the ET biosynthetic pathway (*S-adenosylmethionine synthase 1 - SAMS1; ACC synthase 2, 3, 6 - ACS2, ACS3, ACS6 and ACC oxidase 2 - ACO2*) as well as the most important RNAi genes (*RNA-dependent RNA polymerase 1 - RDR1, Dicer-like 3a - DCL3a, Argonaute 2a, 18a - AGO2a, AGO18a*) in the virus control (Table A.2). Based on preliminary experiments, these genes appeared to be the most suitable for performing measurements under the given experimental settings.

2.6. Metabolomic analysis of ACC

The experiment was performed using a Shimadzu GCMS-TQ 8040 instrument. During sample preparation, 100 mg of plant tissue was homogenized in liquid nitrogen. After adding 30 μl Ribitol (1 mg/ml; internal standard) and 500 μl MeOH the extraction was performed with MiniG (1500 S/minute) and the samples were centrifuged (10,000 rpm, 5 min). After collecting the supernatant, 500 μl of MeOH:H$_2$O (1:1 v:v) was added, extraction was carried out with MiniG (1500 S/minute) and the samples were centrifuged

Table A2

Properties of the forward (F) and reverse (R) primers designed for the reference genes and the genes used for gene expression studies, and the efficiency of the RT-qPCR reactions performed with them (*Folylpolyglutamate synthase* – FPGS, *leunig* – LUG, *S-adenosylmethionine* synthase – SAMS, *ACC synthase* – ACS, *ACC oxidase* – ACO, *RNA-dependent RNA polymerase* – RDR, *Dicer-like* – DCL, *Argonaute* – AGO; *MaizeGDB, ** GenBank).

Gene name	Primer sequences 5′ → 3′	Amplicon length (bp)	Database reference number	Reaction efficiency
FPGS	F – ATCTCGTTGGGGATGTCTTG R – AGCACCGTTCAAATGTCTCC	132	GRMZM2G393334*	1.928 ± 0.027
LUG	F – TCCAGTGCTACAGGGAAGGT R – GTTAGTTCTTGAGCCCACGC	178	GRMZM2G425377*	1.846 ± 0.026
SAMS1	F – CATTGAGCAGCAGTCCCCT R – GGTCTCGTCAGTCGCATAC	117	BT054969**	1.930 ± 0.036
ACS2	F – GACCTCATCCACATCGCGTA R – TCCATCCACGAGAAGAGCC	305	GRMZM2G164405*	1.905 ± 0.021
ACS3	F – TGCCATCACCTTACTACCC R – CACAACATCTGCCACGCTA	332	GRMZM2G018006*	1.884 ± 0.034
ACS6	F – AGGTTCATGTCGGAGCAACG R – TAGTATGGCGTGGGGATGAG	146	GRMZM2G054361*	1.985 ± 0.031
ACO2	F – CAACGGCAGGTAGAAGAGC R – TGTAGAAGGACCCGATGGAC	80	GRMZM2G007249*	1.991 ± 0.054
RDR1	F – GTTTGCTTCTCGGCAGGGAT R – TCGTTCCACCTCAGATTTGTGT	157	GRMZM2G481730*	1.884 ± 0.020
DCL3a	F – GACCTGTGGATTCTACTCTGGA R – ACCCTTGGATGACTTGTTGG	191	JX504672.1**	1.941 ± 0.030
AGO2a	F – CGATTTGGGATTTCCTTGGATG R – CGATACTCAATTTGGAGGTCTG	112	GRMZM2G007791*	1.904 ± 0.042
AGO18a	F – GAAGCTGGTGTCCGAGAACC R – CTACCTCCTTTCCATCCTGC	148	GRMZM2G105250*	1.978 ± 0.055

again (10,000 rpm, 5 min). After separating the supernatant, 500 μl of MQ water was added, and extraction with MiniG (1500 S/minute) was followed by a third centrifugation (10,000 rpm, 5 min). After combining the phases, 50 μl of sample was evaporated for derivatization. After the addition of 40 μl of methoxyamine hydrochloride in pyridine (20 mg/ml) the samples were shaken at 300 rpm for 90 min and then for a further 30 min after the addition of 60 μl of MSTFA (*N*-methyl-N- [trimethylsilyl] trifluoroacetamide). Shaking took place on a heated Eppendorf shaker with incubation at 37°. The GCMS-TQ measurement parameters were as follows: 1 μl was injected onto the column (HP-5MS UI column, 30 m long, 0.25 μm film thickness and 0.25 mm internal diameter) at 230 °C, while the temperature of the transfer line and ion source was 250 °C. The carrier gas was He with a constant flow rate (1 mL/minutes). Temperature program: 70 °C (1 min), 320 °C (3 min), monitoring components in MRM mode. Both GC analysis and data processing were carried out using GCMSSolution 4.16 for Shimadzu.

2.7. Statistical analysis

Four independent experiments were performed with exactly the same parameters to eliminate biological variation. Chlorophyll content and basic growth parameters were sampled in all four biological experiments with 10 technical repeats, while chlorophyll *a* fluorescence measurements, NPQ and gene expression measurements were sampled from three different experiments with 10, 3 and 5 technical replicates, respectively. The virus number studies (ELISA and PrimeTime) and ACC content measurements were performed in 2 biological and 9 or 5 technical replicates, respectively.

The results were statistically evaluated with ANOVA and Tukey's honest significant difference (TukeyHSD) post-hoc test at the 5% significance level ($p \leq 0.05$) using the RStudio program package (Racine, 2012).

3. Results

3.1. Changes in growth parameters and chlorophyll content

Early MDMV-like symptoms appeared on the virus-infected plants as early as three days after the first inoculation. By the third sampling time, the chlorotic spots formed regular streaks, and the retarded growth of infected plants not given siRNA pre-treatment was also significant (Fig. A.1).

In order to monitor the physiological condition of the plants, examinaitons were first made on the effects of viral infection, with or without pre-treatment with siRNA, on basic growth parameters, including the measurement of length, fresh and dry weight of both shoots and roots (Fig. 1). Measurements were taken one, two, and three weeks after the first inoculation. From the second week onwards the values recorded for the shoots of *siRNA-Inf* plants were higher than those for infected plants without pre-treatment (group *Inf*). This difference was significant for the length, fresh and dry weight of the shoots, and for the fresh and dry root weight of the *siRNA-Inf* group by the third week. By this time, the values of this group were close to those of the control groups (*Co, siRNA*), while the values of the *Inf* group were significantly lower. Although no large differences were found in the root length data, the advantage of the *siRNA-Inf* group was also seen in the fresh and dry root weights 3 weeks after infection.
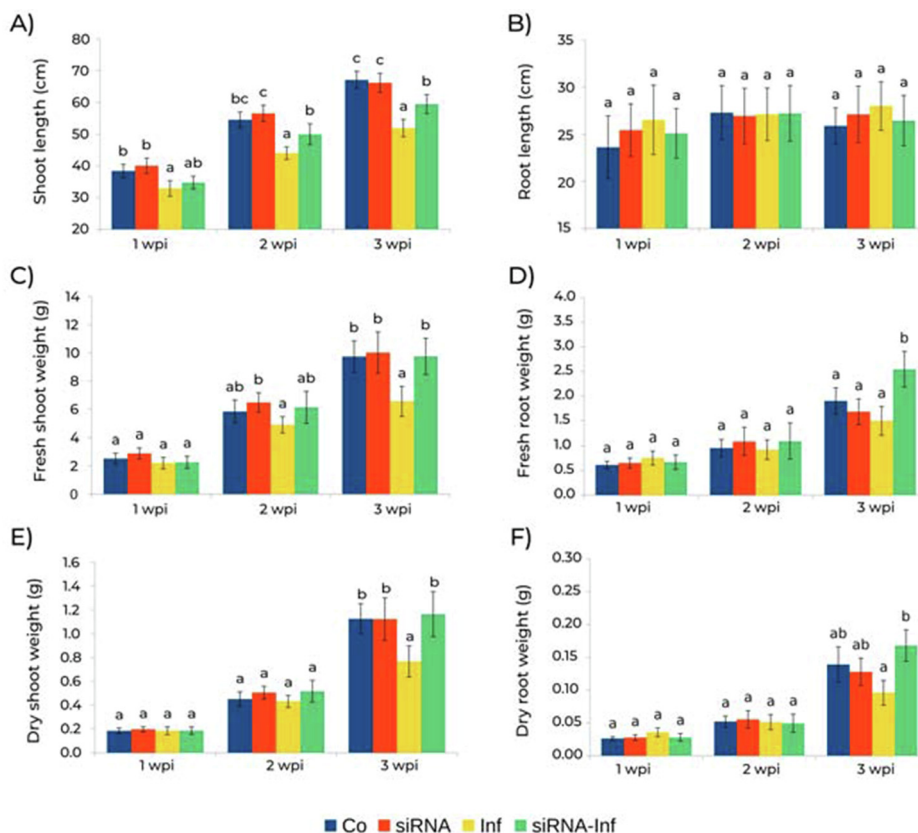

Fig. 1. Length, fresh and dry weights of shoots and roots in the different treatment groups (*Co* – control, *siRNA* – small RNA- treated, *Inf* – MDMV-infected and *siRNA-Inf* – small RNA pre-treatment followed by MDMV infection; wpi – weeks post infection; error bars represent standard deviation and different letters indicate significant differences at p ≤ 0.05).

Changes in chlorophyll content were also monitored. Following plant growth, the third, fourth, fifth, sixth and seventh leaves were also examined over the three-week period of the experiment. The results showed a similar trend in this case as well, the values of the *siRNA-Inf* group being significantly higher compared to the *Inf* group (Fig. 2). In addition, this parameter also highlighted the developmental delay of MDMV-infected plants. No fifth leaves were present in the *Inf* group in the first week after the infection, or they were so small that they could not be measured reliably (Fig. A.1), while the fifth leaves of the *siRNA-Inf* group plants were visibly better developed and their SPAD values approached the average of the control groups (Fig. 2C). In group *siRNA,* the small RNA treatment had no effect on either growth parameters or chlorophyll content, suggesting that treatment without stress did not significantly affect the plant. In contrast, pre-infection siRNA treatment may have successfully alleviated the degree of stress caused by viral infection, as evidenced by the improved condition of the *siRNA-Inf* group for these parameters.

3.2. Changes in chlorophyll fluorescence and non-photochemical quenching parameters

An examination of the maximum and actual quantum efficiency of PSII reaction centres provides an even more nuanced picture of the instantaneous physiological state of the plants. The F_v/F_m ratio indicates the maximum quantum efficiency of dark-adapted PSII reaction centres, while $\Delta F/F_m'$ stands for the actual quantum efficiency of the light-adapted PSII reaction centres. For many types of stress, these ratios have been shown to be a reliable indication of changes in plant physiological status. However, no salient changes were observed in the present experimental setup due to either MDMV infection, small RNA treatment or dual treatment (Fig. A.2, Fig. A.3). There was no change in NPQ parameters as a result of small RNA treatment, while a significant decrease in the Φ_{PSII} parameter was continuously observed in group *Inf* over the

three-week duration of the experiment compared to the control groups. In parallel, the Φ_{NF} values of this same group increased significantly (Fig. 3). In contrast, a lower degree of PSII inactivation was recorded for plants in the *siRNA-Inf* group, indicated by significantly higher Φ_{PSII} and significantly lower Φ_{NF} and Φ_{NPQ} values by the second and third week compared to the *Inf* group (Fig. 3C).

3.3. Quantification of virus particles in the leaves of infected plants

Two approaches were used to check the success of viral infection and to quantify particles of viral origin. Changes in viral RNA levels were monitored with RT-qPCR-based analysis and changes in viral coat protein levels with DAS-ELISA over a three-week period. Both the appearance of visible symptoms and these measurements demonstrated that the inoculations were successful, as viral RNA and coat protein were detectable in plants in the *Inf* and *siRNA-Inf* groups, but could not be detected in uninfected plants. In the first week the decrease in viral RNA was more pronounced, but the amount of coat protein in *siRNA-Inf* was also significantly lower than in *Inf* (Fig. 4). By the second and third weeks, the amount of viral RNA increased in *siRNA-Inf*, but did not reach the value from the *Inf* group on either occasion. Similarly, the amount of coat protein remained significantly lower in the *siRNA-Inf* group compared to *Inf*. The efficiency of siRNA pre-treatment is indicated by the fact that neither the RNA nor the coat protein levels reached those experienced in *Inf* during the three weeks.

3.4. Analysis of gene expression in maize

In the first week the gene expression of protein genes involved in the process of RNAi was influenced by siRNA treatment alone. In the siRNA group, RDR1, DCL3a and AGO2a showed a 1.5-fold increase, while AGO18a was the most prominent with an approximately 4-fold increase in expression (Fig. 5). As a result of MDMV infection, the transcription of the RDR1 and DCL3a protein genes
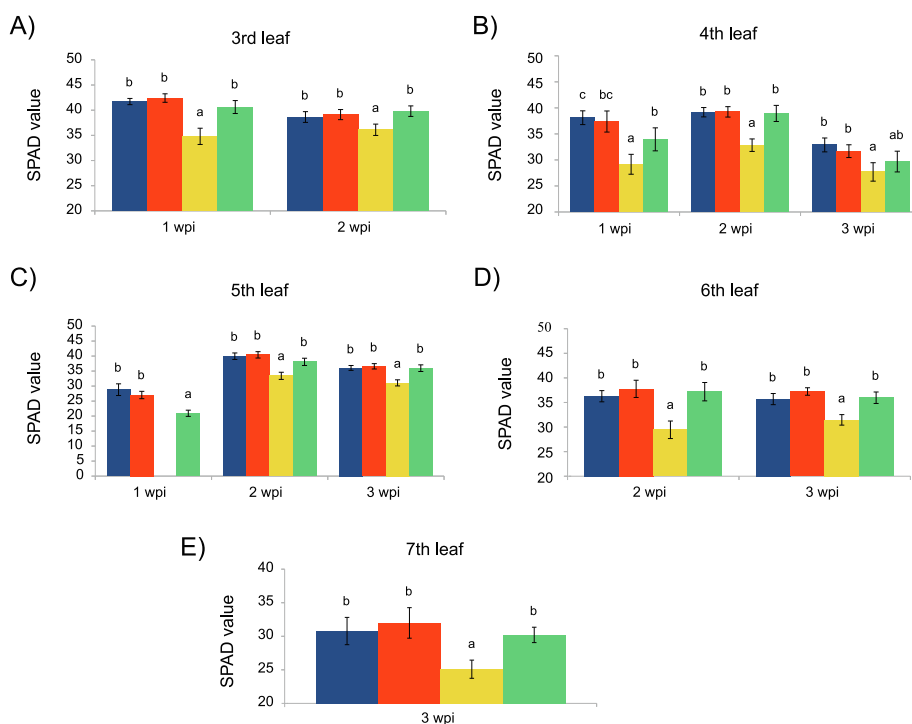

Fig. 2. Changes in chlorophyll contents estimated with SPAD values in the *Co* and *Inf* leaves with or without siRNA treatment. During the first week, the fifth leaf of the plants in group *Inf* was missing or so small that it could not be measured reliably. (*Co* – control, *siRNA* – small RNA-treated, *Inf* – MDMV-infected and *siRNA-Inf* – small RNA pre-treatment followed by MDMV infection; wpi – weeks post infection; error bars represent standard deviation and different letters indicate significant differences at p $\leq$ 0.05).
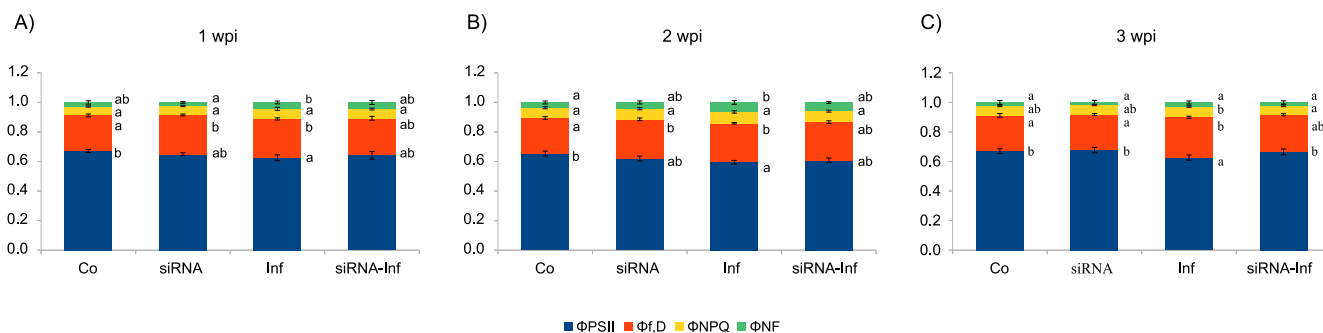
Fig. 3. Differences in NPQ parameters measured one (A), two (B) and three (C) weeks after infection *(Co* – control, *siRNA* – small RNA-treated, *Inf* – MDMV-infected and *siRNA-Inf* – small RNA pre-treatment followed by MDMV infection; Φ_{PSII} - photochemical efficiency of functional PSII centres; $\Phi_{f,D}$ - fluorescence/thermal dissipation of the absorbed energy; Φ_{NPQ} – pH- dependent, xanthophyll cycle-coupled non-photochemical quenching; Φ_{NF} - thermal dissipation by inactive PSII centres; wpi – weeks post infection; error bars represent standard deviation and different letters indicate significant differences at $p \le 0.05$).
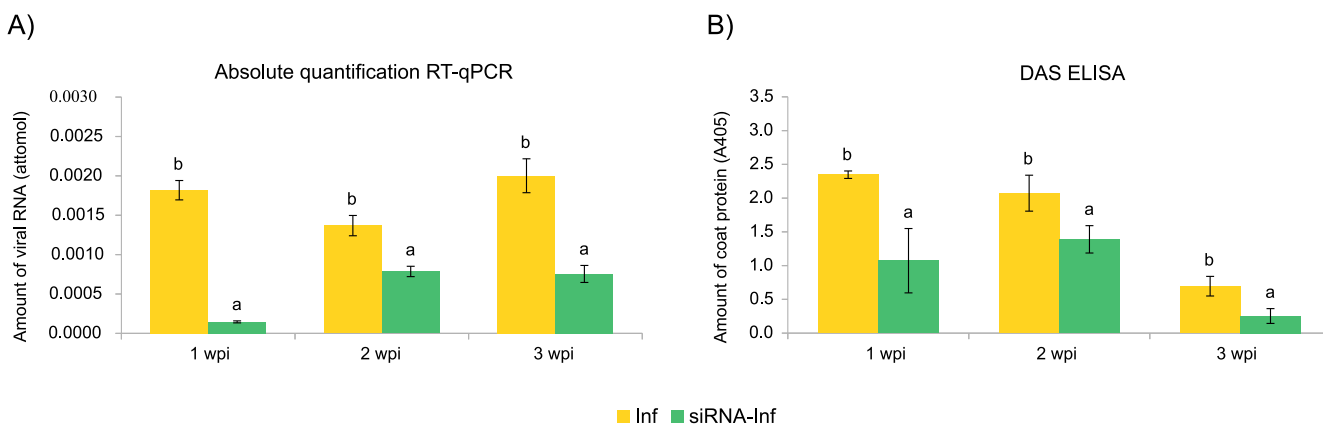

Fig. 4. Quantitative changes in MDMV RNA (A) and coat protein (B) in leaves of siRNA-pretreated maize at 1, 2 and 3 weeks post-infection. The values of the *siRNA-Inf* group are represented as a percentage of the mean Inf group values (wpi – weeks post-infection; error bars represent standard deviation and the different letters indicate significant differences at $p \le 0.05$).

involved in the initial stage of RNAi was significantly higher than in the siRNA and Co groups, with an approximately 3-fold increase. The largest changes were seen for the AGO genes, where the expression increased approximately 7-fold in *AGO2a* and approximately 35-fold in *AGO18a* compared to the values of the control groups. However, in the *siRNA-Inf* group, an even larger, significant increase was observed for the studied genes. The expression of the *RDR1*, *DCL3a* and *AGO2a* genes decreased by the second and third weeks, when the increase was not more than 2.5-fold in either treatment group, while the expression of *AGO18a* remained higher, showing a minimum 15-fold increase in *Inf*, suggesting its important role in the control of MDMV infection (Fig. A.4).

In order to investigate the effect of siRNA treatment and viral infection on the ET biosynthetic pathway, changes in the expression of genes responsible for the production of ET hormone were investigated (Fig. 6). One week after the treatments the transcription levels of the *SAMS1* gene, encoding the enzyme responsible for the initial step of the pathway, was significantly increased by viral infection compared to the control groups, while in the *siRNA-Inf* group its value remained at the control level. Among the genes encoding the ACS protein responsible for SAM - ACC transformation, *ACS2* and *ACS6* changed to the greatest extent, exhibiting distinct gene expression patterns in the *Inf* and *siRNA-Inf* groups. As the result of viral infection, the transcription level of these genes increased significantly, almost twofold for *ACS2* and more than 10-fold for *ACS6*. In contrast, their gene expression in the *siRNA-Inf* group was close to the control values and proved to be significantly lower than in *Inf*. The transcription of the *ACO2* protein gene,

which is responsible for the last step in the biosynthetic pathway, i.e. the formation of ET, was permanently increased by viral infection, with a more than 2-fold increase at 1 wpi. However, plants pre-treated with siRNA had lower transcription levels over the three weeks, representing a significant change in favour of the *siRNA-Inf* group. In the second and third weeks, neither the *SAMS1* nor the *ACS* genes showed an increase greater than 1.5-fold. In the *Inf* and *siRNA-Inf* groups the values either remained close to those of the control groups (e.g., *SAMS1*) or were even significantly lower (e.g. *ACS6*). The transcriptional levels of ACO2 showed a slight increase 2 and 3 weeks after treatment in the *Inf* group, while remaining significantly lower in the *siRNA-Inf* group. It is also worth noting that siRNA treatment significantly reduced the expression of the *ACS2* and *ACS6* genes one and two weeks after infection, respectively (Fig. 6).

The results of gene expression studies thus revealed that genes involved in the process of RNAi were activated in the youngest leaves of virus-infected maize. The RNAi genes exhibited even more pronounced expression in the siRNA-pretreated group, suggesting the development of stronger viral defence. The transcription of most genes in the ET biosynthetic pathway was also increased by viral infection, whereas siRNA treatment and siRNA pre-treatment tended to decrease the expression activity of these genes. Genes involved in the ET biosynthetic pathway showed lower levels of transcription, although significantly higher values were characteristically obtained after infection in the *Inf* group than in the control and small RNA pre-treatment groups.
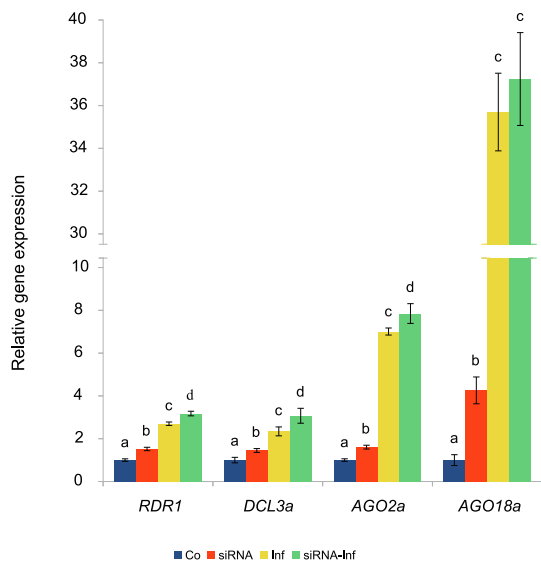
Fig. 5. Gene expression changes of *RNA-dependent RNA polymerase 1* (*RDR1*), *Dicer-like 3a* (*DCL3a*) and *Argonaute 2a, 18a* (*AGO2a, AGO18a*) in the different treatment groups 1 week after the infections (*Co* – control, *siRNA* – small RNA treated, *Inf* – MDMV infected and *siRNA-Inf* – small RNA pretreated and then MDMV infected groups; wpi – weeks post infection. The control value is 1, error bars represent standard deviation and the letters indicate statistically significant difference, $p \leq 0.05$).

3.5. Changes in the amount of ACC

In addition to the expression analysis of ET biosynthetic pathway genes, the direct precursor of ET was also analysed usign gas chromatography. During the three-week experiment, the quantity of ACC decreased over time in the *Inf* and *siRNA-Inf* groups (Fig. 7), while neither the *Co* nor the *siRNA* groups accumulated ACC to any great extent over the three-week period. However, the amount of ACC increased significantly as a result of infection, as indicated by the significantly higher value in the *Inf* group compared to the control groups in the first and second weeks. The *siRNA-Inf* group also exhibited a metabolite peak in the first week, but this was already significantly lower than in the Inf group by the second week. Three weeks after infection, higher ACC accumulation was not observed in either group.

4. Discussion

The physiological condition of plants is significantly affected by viral infections. Viral proliferation occurs at the expense of the energy and protein stores in infected plant cells. At the same time, plants invest much of their remaining resources in the fight against infection, making them even less capable of maintaining growth. Viral replication takes place in the indentations of the membranes of individual plant cell organelles, such as the endoplasmic reticulum and chloroplast (Rajamäki et al. 2004; Csorba et al. 2015). This poses an additional problem, as damage to the outer membranes of chloroplasts leads to damage to the structure of the thylakoid membrane system, resulting in a decrease in chlorophyll content and a deterioration in the efficiency of photosynthetic processes. The resulting lack of energy and reducing capacity causes a decrease in photoassimilation, which is manifested in the dwarf growth that indicates a decrease in plant biomass (Wei et al. 2010). Transmission electron microscopy studies on manioc plants infected with ACMV (*African cassava mosaic virus*) demonstrated that the chloroplasts of virus-infected plants contained much smaller thylakoids with fewer grana than control plants, combined
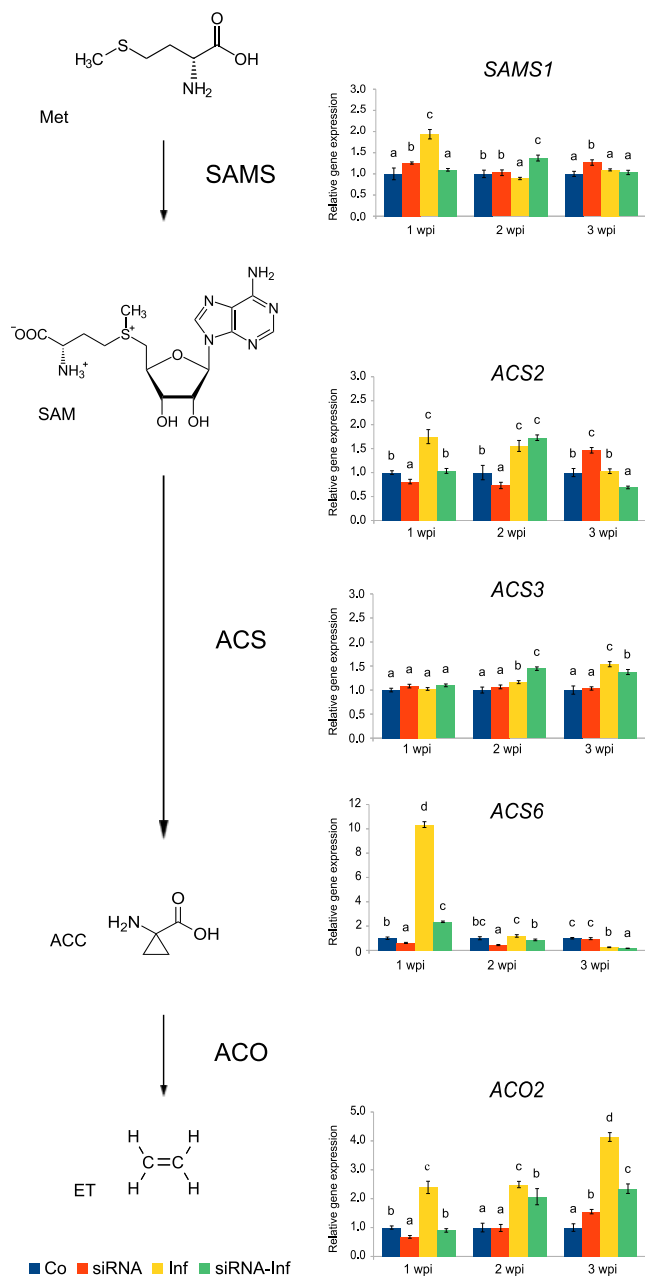

Fig. 6. Gene expression changes in *S-adenosylmethionine synthase 1* (*SAMS1*), *ACC synthase 2, 3, 6* (*ACS2, ACS3, ACS6*) and *ACC oxidase 2* (*ACO2*) in the different treatment groups 1, 2 and 3 weeks after infection (*Co* – control, *siRNA* – small RNA-treated, *Inf* – MDMV-infected and *siRNA-Inf* – small RNA pre-treatment followed by MDMV infection; wpi – weeks post infection. The control value was 1. Different letters indicate significant differences at $p \leq 0.05$).

with significantly lower chlorophyll (Liu et al. 2014). Similarly, when (Cueto-Ginzo et al., 2016) Serrano et al. (2016) inoculated maize plants with MDMV and examined changes in chlorophyll content, photosynthetic efficacy and shoot length, they found a clear reduction in chlorophyll content and photosynthetic efficacy in infected plants compared to control plants. In parallel, shoot length values proved to be significantly lower in the control group. This is in agreement with the present results, where MDMV infection also reduced the chlorophyll content in maize plants. The chlorophyll content of the youngest leaves in the *Inf* group was significantly lower than in the *Co* and *siRNA* groups. In contrast, significantly higher values were observed in groups treated with siRNA before infection (Fig. 2).
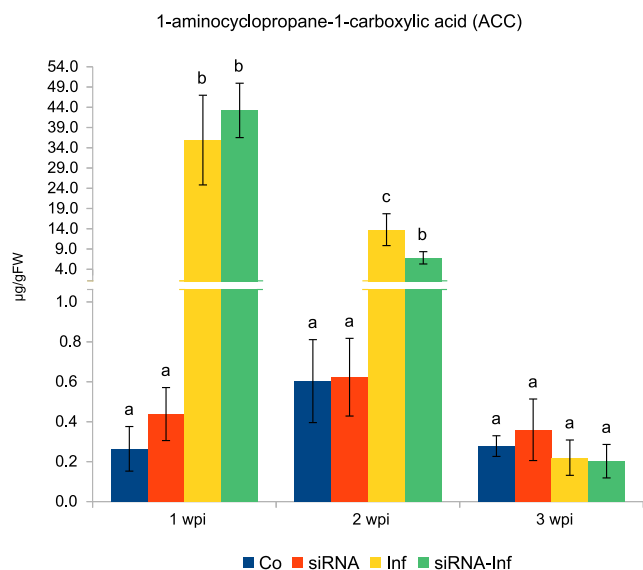
Fig. 7. Changes in the amount of ACC one, two, and three weeks after infection (*Co* – control, *siRNA* – small RNA-treated, *Inf* – MDMV-infected and *siRNA-Inf* – small RNA pre-treatment followed by MDMV infection; wpi – weeks post infection. The control value was 1. Error bars represent standard deviation and different letters indicate significant differences at p ≤ 0.05).

In the present experiments the infected plants showed phenotypic stripes typical of MDMV infection. Chlorotic spots appeared as early as three days after the second infection, while dwarf growth peaked in the third week compared to the other groups. In the first week, no great differences were observed between the individual treatments in the basic growth parameters of the seedlings. However, the values obtained in the second and third weeks were already significantly lower in the virus-infected group, while the groups pretreated with siRNA molecules showed the same values as the control groups (Fig. 1). By the third sampling date, plants in the *Inf* group had significantly lower shoot length, fresh and dry shoot weight, and fresh and dry root weight compared to the control groups, while plants in the *siRNA-Inf* group showed significantly better values.

The encouraging results obtained for the physiological measurements were supported by the quantification of virus particles. Over the three-week period significantly lower viral RNA and coat protein levels were detected in the youngest leaves of plants in the *siRNA-Inf* group (Fig. 4). The effect of pre-infection siRNA treatment appeared to be greatest in the first week. Although the amount of both viral RNA and capsid increased by the second and third weeks, it never reached the level of the *Inf* group. Decreased viral RNA and coat protein content presumably results in less virus accumulation

in the younger leaves. Numerous authors have suggested that treatment with siRNA or longer dsRNAs can help to reduce the amount of virus and thus alleviate the symptoms of viral infection (Konakalla et al. 2016, Mitter et al. 2017, Kaldis et al. 2018). The background of these results is primarily explained by the activation of the viral defence system of the plants, the process of RNAi.

During viral replication in the cytoplasm of the plant cell, exogenous RNA or DNA released from the coat protein subunits serves as a signal to the plant, resulting in the immediate activation of the RNAi process. Proteins encoded by the *RDR1* and *RDR6* genes are thought to be responsible for the formation of double-stranded RNA, which can then be diced to secondary siRNA molecules during geminiviral infection in *Arabidopsis thaliana* (Guo et al. 2019). The dsRNAs formed by RDRs are then cleaved by DCL proteins, specifically into 21–24-nucleotide siRNA duplexes. In the case of *Tomato yellow leaf* curl *virus* (TYLCV) infection in tomato (*Solanum lycopersicum*), the *DCL2* gene product is responsible for the formation of this viral siRNA in cooperation with RDR6. AGO1 and AGO4 play a role in siRNA-driven TYLCV inheritance, binding, and cleavage by AGO-RISC (RNA-induced silencing complex) (Bai et al. 2012). In addition to *AGO2*, *AGO1* homologues were found to be crucial in the defence mechanism against wild-type *Turnip crinkle virus* (TCV) in *Nicotiana benthamiana* (Ludman and Fátyol, 2020). During MDMV infection, a moderate increase in the expression of the *RDR1* and *DCL3a* genes responsible for the initial steps of RNAi was recorded in the present work. Among the genes coding for the AGO proteins responsible for processing the siRNAs formed, *AGO2a* and *AGO18a* showed an outstanding increase in gene expression (Fig. 5). The gene of the monocot-specific AGO18 protein responds to viral infections, plays a major role in antiviral defence of infected tissues and has a regulatory role in antiviral RNAi (Wu et al. 2015, Chen and Ding 2020). Pre-infection small RNA treatment had a priming effect on the system, so that the previously activated RNAi process gave a more intense response to the cytoplasmic appearance of MDMV RNA. Infection thus presented a lower initial load in the *siRNA-Inf* group, allowing the plants to devote more energy to their growth, development and defence, resulting in better physiological status than in plants in the *Inf* group.

Plant hormone ET also plays an important role in plant-virus interactions. It has recently been discovered that ET production can be stimulated by certain viruses, such as the *Rice dwarf virus* (RDV). In RDV-infected rice plants ET production increased as a consequence of direct SAMS induction, making the plants more susceptible to the virus, which then spread more efficiently (Zhao et al. 2017). Other experiments showed that the effect of ET signalling may help viral infection by reducing the protection of plants against viral vectors (Casteel et al. 2015) or even by stimulating the attraction of vectors (Bak et al. 2019). The effect of MDMV infection and siRNA pre-treatment on the ET biosynthetic

Fig. A1. Photographs of experimental plants one week after siRNA treatment and infection. Numbers indicate the corn leaves in different developmental stages (Co – control, siRNA – small RNA-treated, Inf – MDMV-infected and siRNA-Inf – small RNA pretreated followed by MDMV infection).
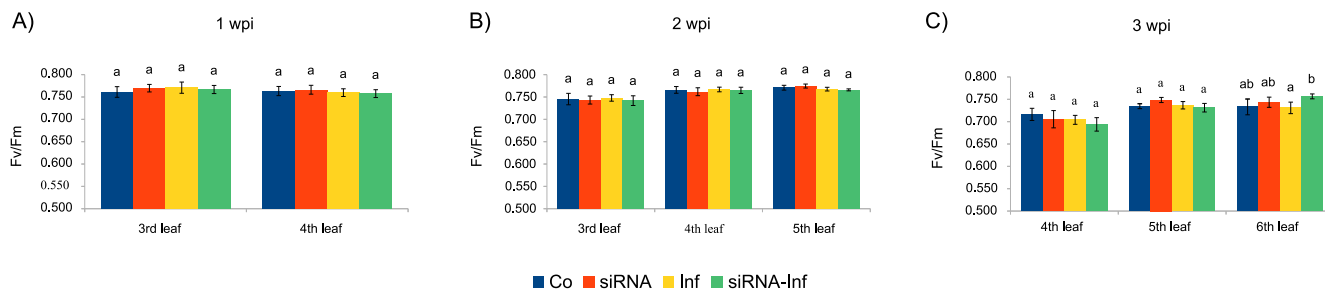
Fig. A2. Changes in the maximum quantum efficiency (Fv/Fm) of PSII reaction centres 1, 2 and 3 weeks after infection (Co – control, siRNA – small RNA-treated, Inf – MDMV-infected and siRNA-Inf – small RNA pretreatment followed by MDMV infection; wpi – weeks post infection; error bars represent standard deviation and different letters indicate significant differences at P ≤ 0.05).
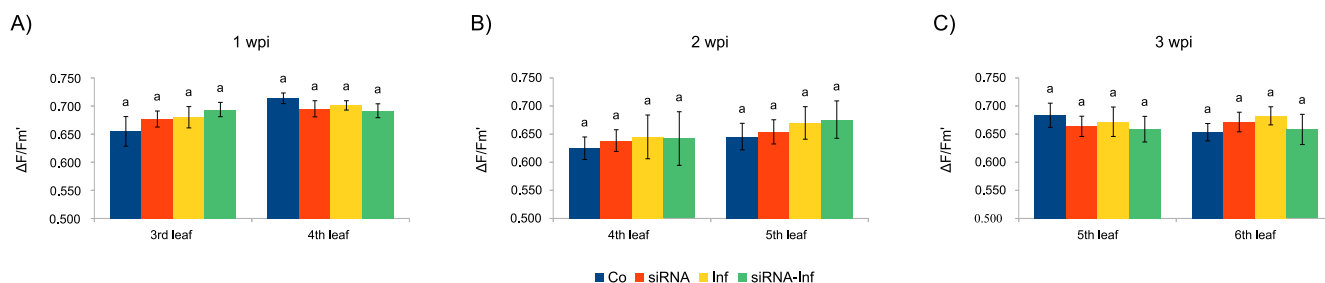

Fig. A3. Changes in the maximum quantum efficiency (ΔF/Fm') of PSII reaction centres in the light-adapted state 1, 2 and 3 weeks after infection (Co – control, siRNA – small RNA-treated, Inf – MDMV-infected and siRNA-Inf – small RNA pretreatment followed by MDMV-infection; wpi – weeks post infection; error bars represent standard deviation and different letters indicate significant differences at P ≤ 0.05).
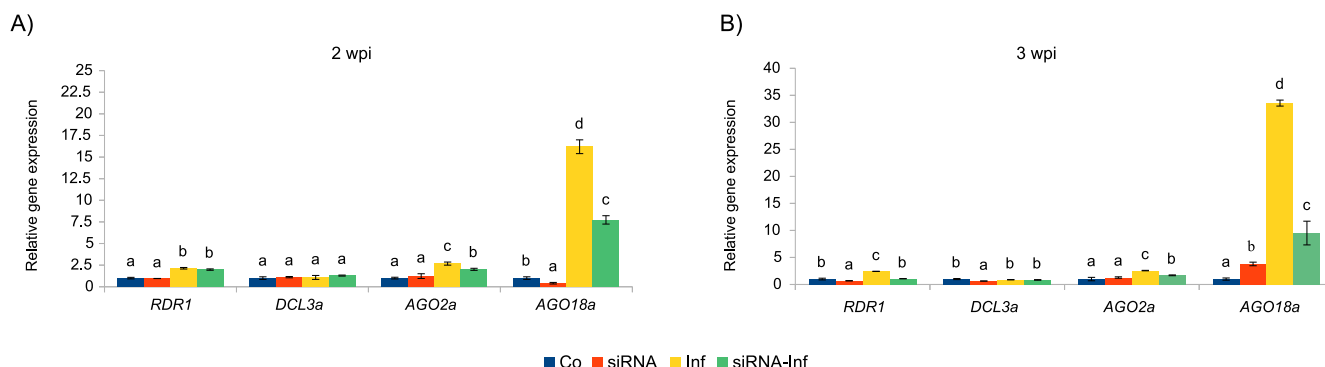

Fig. A4. Gene expression changes in RNA-dependent RNA polymerase 1 (RDR1), Dicer-like 3a (DCL3a) and Argonaute 2a, 18a (AGO2a, AGO18a) in the different treatment groups 2 and 3 weeks after infection (Co – control, siRNA – small RNA-treated, Inf – MDMV-infected and siRNA-Inf – small RNA pretreatment followed by MDMV infection; wpi – weeks post infection. The control value was 1. Error bars represent standard deviation and different letters indicate significant differences at p ≤ 0.05.)

pathway was monitored by examining the transcription level of the protein genes and quantitative changes in the ACC metabolite. It can be stated that MDMV infection significantly increased the expression of the *SAMS1*, *ACS2*, *ACS6* and *ACO2* genes, which was not altered or possibly reduced by siRNA treatment (Fig. 6). Due to the increased transcription of *SAMS1*, *ACS2* and *ACS6*, a larger amount of ACC accumulation was expected during the first week in the *Inf* group, especially as a metabolite peak was detected in MDMV-infected plants during metabolomic measurements on ACC (Fig. 7). Nevertheless, despite the reduced expression, a significantly higher accumulation of ACC was also measured in siRNA-pretreated plants compared to the control groups. One explanation could be the translational modification of ACSs through phosphorylation, leading to enhanced ACC activity due to the greater stability of the enzyme (Van de Poel and Van Der Straeten, 2014). In *Arabidopsis AtACS6* is a type-1 ACS enzyme with phosphorylation sites for CDPK and MAPK kinases (Argueso et al. 2007). The increased protein stability following phosphorylation could

decrease the expression of the coding gene through negative feedback regulation (Park et al. 2021). In the present case, the applied siRNA treatment may have influenced the phosphorylation level of ACS6, resulting in an increased half-life. This negative feedback might contribute to the decreased gene expression observed (Fig. 6). A second option is that the virus stimulates the synthesis of polyamines through SAM. The conversion of SAM to ACC is a plant strategy aimed at preventing the use of polyamines by viruses for their transcriptional and translational processes (Firpo and Mounce, 2020). In the maize-MDMV interaction the plants pre-treated with siRNA were able to suppress virus replication resulting in the reduction of polyamne synthesis and more SAM to convert into ACC by ACS enzymes. Whereas in infected plants polyamines are produced and the cells try to convert as much SAM as possible during infection to resist virus replication. These two options might be linked and could form a third explanation in combination with other aspects. Due to siRNA pre-treatment the *siRNA-Inf* plants gave a more distinct response to viral infec-

tion, including higher RNAi gene expression levels. Thus, as a primed stress response, phosphorylation of ACS6 could happen earlier in siRNA-Inf plants. Given the longer protein turnover and a possible previously achieved ACC concentration peak might emerge a negative feedback loop, which decreased *ACS6* expression at 1 wpi. In *Inf* plants these steps happened several days later, as indicated by the higher expression of *ACS6* one wpi and significantly higher ACC content two wpi compared to the *siRNA-Inf* group. Judging by the changes in ACC content, there was a constant gradual decrease in both the *Inf* and *siRNA-Inf* groups, and a constant increase in *ACO2* expression throughout the three-week period. This may have contributed to constant ET synthesis and/or to the formation of inactive ACC-conjugates. The *ACO2* expression in *siRNA-Inf* plants was significantly lower, suggesting a lower rate of ET production. However, the ACC supply for ET synthesis seems to have decreased over time, suggesting the down regulation of this metabolic pathway in the *siRNA-Inf* compared to *Inf* group.

5. Conclusions

As a result of small-RNA treatment, a priming process was started in the plant, which resulted in a more intense stress response. Thus, infected plants pretreated with siRNA were in better physiological condition by the end of the experiment than those infected without pre-treatment. The lower initial amount of virus meant a weaker stress load, which allowed the plants to devote more energy to growth and development. This protective effect was also seen at the molecular level, as the amount of viral RNA and coat protein was significantly reduced by the stronger activation of the defence system caused by the pre-treatment. In contrast, siRNA pre-treatment did not initially affect the quantitative change in ACC and thus in ET, though later a significant decrease was detected. Moreover, the ET biosynthetic pathway appeared to be considerably down-regulated during infection due to the siRNA pre-treatment. In combination with the significantly better physiological condition, the enhanced RNAi response and the lower quantity of virus particles in siRNA-pretreated plants, it can be concluded that siRNA pre-treatment stimulated the antiviral defence of MDMV- infected plants. In addition, the better physiological condition and the consistently lower ACC content of the *siRNA-Inf* group suggest that ET does not significantly contribute to the successful defence in this maize hybrid type against MDMV.

6. Code availability

All software applied in this study are cited in this published article.

7. Availability of data and material

All data generated or analysed during this study are included in this published article.

8. Consent for publication

Manuscript is approved by all authors for publication. All the authors listed have approved the manuscript that is enclosed.

Declaration of Competing Interest

The authors declare that they have no known competing financial interests or personal relationships that could have appeared to influence the work reported in this paper.

References

Adams, D.O., Yang, S.F., 1977. Methionine metabolism in apple tissue. Plant Physiol. 60 (6), 892–896. https://doi.org/10.1104/pp.60.6.892.

Adams, D.O., Yang, S.F., 1979. Ethylene biosynthesis: Identification of 1-aminocyclopropane-1-carboxylic acid as an intermediate in the conversion of methionine to ethylene. Proceedings Natl Acad Sci. 76 (1), 170–174. https://doi.org/10.1073/pnas.76.1.170.

Alazem, M., Lin, N.-S., 2015. Roles of plant hormones in the regulation of host – virus interactions. Mol. Plant Pathol 16 (5), 529–540. https://doi.org/10.1111/mpp.2015.16.issue-510.1111/mpp.12204.

Argueso, C.T., Hansen, M., Kieber, J.J., 2007. Regulation of ethylene biosynthesis. J. Plant Growth Regulation. 26 (2), 92–105. https://doi.org/10.1007/s00344-007-0013-5.

Asiimwe, T., Stewart, L.R., Willie, K., Massawe, D.P., Kamatenesi, J., Redinbaugh, M. G., 2020. Maize lethal necrosis viruses and other maize viruses in Rwanda. Plant. Pathol. 69 (3), 585–597. https://doi.org/10.1111/ppa.v69.310.1111/ppa.13134.

Bai, M., Yang, G., Chen, W., Mao, Z., Kang, H., Chen, G., Yang, Y., Xie, B., 2012. Genome-wide identification of Dicer-like, Argonaute and RNA-dependent RNA polymerase gene families and their expression analyses in response to viral infection and abiotic stresses in Solanum lycopersicum. Gene. 501, 52–62. https://doi.org/ 10.1016/j.gene.2012.02.009

Bak, A., Patton, M.F., Perilla-Henao, L.M., Aegerter, B.J., Casteel, C.L., 2019. Ethylene signaling mediates potyvirus spread by aphid vectors. Oecologia 190, 139–148. https://doi.org/10.1007/s00442-019-04405-0.

Boller, T., Herner, R.C., Kende, H., 1979. Assay for and enzymatic formation of an ethylene precursor, 1-aminocyclopropane-1-carboxylic acid. Planta 145 (3), 293–303. https://doi.org/10.1007/BF00454455.

Broekgaarden, C., Caarls, L., Vos, I.A., Pieterse, C.M.J., Van Wees, S.C.M., 2015. Ethylene: traffic controller on hormonal crossroads to defense. Plant Physiol. 169, 2371–2379. https://doi.org/10.1104/pp.15.01020.

Casteel, C.L., De Alwis, M., Bak, A., Dong, H., Whitham, S.A., Jander, G., 2015. Disruption of ethylene responses by *Turnip mosaic virus* mediates suppression of plant defense against the Green peach aphid vector. Plant Physiol. 169 (1), 209–218. https://doi.org/10.1104/pp.15.00332.

Chen, L., Zhang, L., Li, D., Wang, F., Yu, D., 2013. WRKY8 transcription factor functions in the TMV-cg defense response by mediating both abscisic acid and ethylene signaling in *Arabidopsis*. PNAS 110 (21), E1963–E1971. https://doi.org/10.1073/pnas.1221347110.

Chen, Z.-Q., Ding, S.-W., 2020. JAcked responses go viral: hormonal regulation of antiviral RNAi. Cell Host Microbe 28 (1), 7–9. https://doi.org/10.1016/j.chom.2020.06.007.

Clark, M.F., Adams, A.N., 1977. Characteristics of the microplate method of enzyme-linked immunosorbent assay for the detection of plant viruses. J. Gen. Virol. 34, 475–483. https://doi.org/10.1099/0022-1317-34-3-475.

Csorba, T., Kontra, L., Burgyán, J., 2015. Viral silencing suppressors: Tools forged to fine-tune host-pathogen coexistence. Virology 479–480, 85–103. https://doi.org/10.1016/j.virol.2015.02.028.

Firpo, M.R., Mounce, B.C., 2020. Diverse functions of polyamines in virus infection. Biomolecules. 10, 1–13. https://doi.org/10.3390/biom10040628.

Guo, Z., Li, Y., Ding, S.-W., 2019. Small RNA-based antimicrobial immunity. Nat Rev Immunol. 19 (1), 31–44. https://doi.org/10.1038/s41577-018-0071-x.

Hamilton, A.J., Bouzayen, M., Grierson, D., 1991. Identification of a tomato gene for the ethylene-forming enzyme by expression in yeast. Proceedings Natl. Acad. Sci. USA 88 (16), 7434–7437. https://doi.org/10.1073/pnas.88.16.7434.

Hendrickson, L., Förster, B., Pogson, B.J., Chow, W.S., 2005. A simple chlorophyll fluorescence parameter that correlates with the rate coefficient of photoinactivation of Photosystem II. Photosynth. Res. 84 (1-3), 43–49. https://doi.org/10.1007/s11120-004-6430-4.

Houben, M., Van de Poel, B., 2019. 1-aminocyclopropane-1-carboxylic acid oxidase (ACO): the enzyme that makes the plant hormone ethylene. Front. Plant Sci. Plant Physiol. 10, 695. https://doi.org/10.3389/fpls.2019.00695.

Jin, Y., Zhao, J.H., Guo, H.S., 2021. Recent advances in understanding plant antiviral RNAi and viral suppressors of RNAi. Current Opinion Virol. 46, 65–72. https://doi.org/10.1016/j.coviro.2020.12.001.

Kannan, M., Ismail, I., Bunawan, H., 2018. Maize dwarf mosaic virus: from genome to disease management. Viruses. 10, 492. https://doi.org/10.3390/v10090492.

Kaldis, A., Berbati, M., Melita, O., Reppa, C., Holeva, M., Otten, P., Voloudakis, A., 2018. Exogenously applied dsRNA molecules deriving from the Zucchini yellow mosaic virus (ZYMV) genome move systemically and protect cucurbits against ZYMV. Mol. Plant Pathol 19 (4), 883–895. https://doi.org/10.1111/mpp.2018.19.issue-410.1111/mpp.12572.

Khraiwesh, B., Zhu, J., Zhu, J. 2012. Role of miRNAs and siRNAs in biotic and abiotic stress responses of plants. Biochimica et Biophysica Acta (BBA) - Gene Regulatory Mechanisms. 1819, 137–148. https://doi.org/ 10.1016/j.bbagrm.2011.05.001

Konakalla, N.C., Kaldis, A., Berbati, M., Masarapu, H., Voloudakis, A.E., 2016. Exogenous application of double-stranded RNA molecules from TMV p126 and CP genes confers resistance against TMV in tobacco. Planta 244, 961–969. https://doi.org/10.1007/s00425-016-2567-6.

Koressaar, T., Remm, M., 2007. Enhancements and modifications of primer design program Primer3. Bioinformatics 23 (10), 1289–1291. https://doi.org/10.1093/bioinformatics/btm091.

Liu, J., Yang, J., Bi, H., Zhang, P., 2014. Why mosaic? Gene expression profiling of African cassava mosaic virus infected cassava reveals the effect of chlorophyll degradation on symptom development. J. Integrative Plant Biol. 56 (2), 122–132. https://doi.org/10.1111/jipb.12133.

Kiruwa, F.H., Mutiga, S., Njuguna, J., Machuka, E., Senay, S., Feyissa, Ti., Ndakidemi, PA., Stomeo, F., 2019. Status and epidemiology of maize lethal necrotic disease in Northern Tanzania. Pathogens. 9, 1–5. https://doi.org/10.3390/pathogens9010004

Ludman, M., Fátyol, K., 2020. Targeted inactivation of the AGO1 homeologues of Nicotiana benthamiana reveals their distinct roles in development and antiviral defence. New Phytologist 229, 1289–1297. https://doi.org/10.1111/nph.16992.

Ludmerszki, E., Chounramany, S., Oláh, C., Kátay, G., Rácz, I., Almási, A., Solti, Á., Bélai, I., Rudnóy, S., 2017. Protective role of S-methylmethionine-salicylate in maize plants infected with Maize dwarf mosaic virus. European J. Plant Pathol. 149, 145–156. https://doi.org/10.1007/s10658-017-1174-0.

Mitter, N., Worrall, E.A., Robinson, K.E., Li, P., Jain, R.G., Taochy, C., Fletcher, S.J., Carroll, B.J., Lu, G.Q.M., Xu, Z.P., 2017. Clay nanosheets for topical delivery of RNAi for sustained protection against plant viruses. Nat. Plants 3, 16207. https://doi.org/10.1038/nplants.2016.207.

Park, C., Lee, H.Y., Yoon, G.M., 2021. The regulation of ACC synthase protein turnover : A rapid route for modulating plant development and stress responses. Current Opinion in Plant Biology. 63, 102046. https://doi.org/ 10.1016/j.pbi.2021.102046

Pattyn, J., Vaughan-Hirsch, J., Van de Poel, B., 2021. The regulation of ethylene biosynthesis: a complex multilevel control circuitry. New Phytol. 229 (2), 770–782. https://doi.org/10.1111/nph.v229.210.1111/nph.16873.

Pfaffl, M.W., 2004. Quantification strategies in real time PCR, in: A-Z of Quantitative PCR, ed: Bustin, S.A., International University Line, CA, La Jolla, pp 87–112.

Racine, J.S., 2012. Rstudio: a platform-independent IDE for r and Sweave. J Applied Eco. 27 (1), 167–172. https://doi.org/10.1002/jae.1278.

Rajamäki, M.L., Mäki-Valkama, T., Mäkinen, K., Valkonen, J.P.T., 2004. Infection with potyviruses, in: Plant-pathogene interactions, ed: Talbot, N.J., Annual Plant Reviews, Blackwell Publishing, pp 68–91.

Ramakers, C., Ruijter, J.M., Deprez, R.H.L., Moorman, A.F.M., 2003. Assumption-free analysis of quantitative real-time polymerase chain reaction (PCR) data. Neurosci. Lett. 339 (1), 62–66. https://doi.org/10.1016/S0304-3940(02)01423-4.

Cueto-Ginzo, I.A., Serrano, L., Sin, E., Rodríguez, R., Morales, J.G., Lade, S.B., Medina, V., Achon, M.A., 2016. Exogenous salicylic acid treatment delays initial infection and counteracts alterations induced by Maize dwarf mosaic virus in the maize proteome. Phys. Mol. Plant Pathol. 96, 47–59. https://doi.org/10.1016/j.pmpp.2016.07.001.

Sastry, K.S., Zitter, T.A., 2014. In: Plant Virus and Viroid Diseases in the Tropics. Springer Netherlands, Dordrecht, pp. 149–480. https://doi.org/10.1007/978-94-007-7820-7_2.

Solti, Á., Gáspár, L., Mészáros, I., Szigeti, Z., Lévai, L., Sárvári, É., 2008. Impact of iron supply on the kinetics of recovery of photosynthesis in Cd-stressed poplar (Populus glauca). Annals of Botany. 102, 771–782. https://doi.org/ 10.1093/aob/mcn160.

Trebicki, P., 2020. Climate change and plant virus epidemiology. Virus Research. 286, 198059. https://doi.org/10.1016/j.virusres.2020.198059.

Van de Poel, B., Van Der Straeten, D., 2014. 1-aminocyclopropane-1-carboxylic acid (ACC) in plants: More than just the precursor of ethylene! Frontiers. Plant Sci. 5, 1–11. https://doi.org/10.3389/fpls.2014.00640.

Ververidis, P., John, P., 1991. Complete recovery in vitro of ethylene-forming enzyme activity. Phytochemistry 30 (3), 725–727. https://doi.org/10.1016/0031-9422(91)85241-Q.

Wei, T., Huang, T.-S., McNeil, J., Laliberté, J.-F., Hong, J., Nelson, R.S., Wang, A., 2010. Sequential recruitment of the endoplasmic reticulum and chloroplasts for plant potyvirus replication. J. Virol. 84 (2), 799–809. https://doi.org/10.1128/JVI.01824-09.

Wijayasekara, D., Ali, A., 2020. Complete genome characterization and coat protein genealogy of isolates of Maize dwarf mosaic virus from johnsongrass and maize in Oklahoma and Missouri. Plant Dis. 104, 1214–1223. https://doi.org/10.1094/PDIS-06-19-1274-RE.

Wu, J., Yang, Z., Wang, Y., Zeng, L., Ye, R., Ji, Y., Zhao, S., Ji, S., Liu, R., Xu, L., Zheng, H., Zhou, Y., Zhang, X., Cao, X., Xie, L., Wu, Z., 2015. Viral-inducible Argonaute18 confers broad-spectrum virus resistance in rice by sequestering a host microRNA. ELife. 4, 1–19. https://doi.org/10.7554/eLife.05733.

Yadav, S.S., Redden, R.J., Hatfield, J.L., Ebert, A.W., Hunter, D., 2019. Pests and diseases under climate change; Its threat to food security. Food Security and Climate Change. Wiley-Blackwell, 229–241.

Zhao, S., Hong, W., Wu, J., Wang, Y., Ji, S., Zhu, S., 2017. A viral protein promotes host SAMS1 activity and ethylene production for the benefit of virus infection. ELife - Plant Biology. 12, 1–22. https://doi.org/10.7554/eLife.27529.001.

Zhang, D.-W., Deng, X.-G., Fu, F.-Q., Lin, H.-H., 2015. Induction of plant virus defense response by brassinosteroids and brassinosteroid signaling in Arabidopsis thaliana. Planta 241 (4), 875–885. https://doi.org/10.1007/s00425-014-2218-8.